

Estimation of optical pathlength through tissue from direct time of flight measurement

D T Delpy, M Cope, P van der Zee, S Arridge, Susan Wray[†] and J Wyatt[‡]

Departments of Medical Physics, [†]Physiology and [‡]Paediatrics, University College London, 1st Floor, Shropshire House, 11-20 Capper Street, London WC1E 6JA, UK

Received 20 May 1988, in final form 22 July 1988

Abstract. Quantitation of near infrared spectroscopic data in a scattering medium such as tissue requires knowledge of the optical pathlength in the medium. This can now be estimated directly from the time of flight of picosecond length light pulses. Monte Carlo modelling of light pulses in tissue has shown that the mean value of the time dispersed light pulse correlates with the pathlength used in quantitative spectroscopic calculations. This result has been verified in a phantom material. Time of flight measurements of pathlength across the rat head give a pathlength of 5.3 ± 0.3 times the head diameter.

1. Introduction

Changes in cerebral oxygenation and metabolism have for a long time been monitored by optical techniques. Such measurements rely upon oxygen dependent absorption changes that occur in tissue caused by natural chromophores, e.g. haemoglobin in the red blood cell and cytochromes a, b, and c in the cell mitochondrial membrane. Because of the intense absorption of visible light by these chromophores, optical monitoring has only been possible using reflected light from the exposed cerebral cortex. However, in 1977 Jöbsis showed that by using near infrared light (NIR), tissue absorption fell sufficiently for transillumination of the intact head of the cat to be possible. In this spectral region (700-1300 nm), the oxygen dependent absorption of haemoglobin is still observable, together with an oxygenation dependent absorption arising from cytochrome aa₃. By measuring absorption changes at several wavelengths it has been possible to monitor continuously the cerebral oxygenation state in many animals (Piantadosi *et al* 1986, Hazeki *et al* 1987) and by operating in reflection mode, on the human adult (Fox *et al* 1985, Ferrari *et al* 1986a) and newborn infant (Brazy *et al* 1985, Ferrari *et al* 1986b). Technical developments of the instrumentation have now made it possible to measure absorption changes across a total of 10 optical densities (OD) equivalent to 8-9 cm of brain tissue (Cope and Delpy 1988). With such instruments it is possible to transilluminate the head of most preterm infants (Wyatt *et al* 1986).

It has previously been demonstrated (Cope *et al* 1988) that when transilluminating a thick section of a highly scattering medium, it is still possible to apply a simple Beer-Lambert calculation to convert the measured variations in attenuation to changes in the absolute concentration of chromophore. However, the optical pathlength used in the calculation must be increased to take into account the effects of multiple scattering. Tissue is an effective multiple scatterer of light, and the pathlength of the

light in the tissue is normally unknown. For this reason, most published observations have been of a qualitative nature. When measuring in transillumination mode, it is, however, possible to know the minimum optical pathlength (i.e. the inter-optode spacing), and hence place an upper limit on the calculated chromophore concentrations. In studies in human neonates, it has been shown that several NIR monitored indices of cerebral oxygen can be quantitated by using additional independently monitored physiological data (Wyatt *et al* 1986, Delpy *et al* 1987, Cope *et al* 1988). Further, in recent studies in rats, the optical pathlength has been estimated by monitoring the height of the water absorption peak at 975 nm and assuming a value for the average water content of brain tissue (Wray *et al* 1988). Calculations based upon this method indicate an average optical pathlength across the rat head that is approximately 4.3 times the inter-optode spacing.

The developments of the synchronously pumped dye laser and the synchroscan streak camera now make possible the generation of intense picosecond duration pulses of light and their detection at very low intensity with approximately 10 picosecond resolution. Using this equipment the time of flight and temporal dispersion of light pulses through a multiple scattering medium can be studied. The transit times (t) of the photons can be converted into distance travelled through the medium (d) using the formula

$$d = \frac{ct}{n} \quad (1)$$

where n is the refractive index of the medium and c the velocity of light in a vacuum. For water ($n = 1.33$) the conversion factor is 0.225 mm ps^{-1} and for tissue ($n = 1.40$, see discussion) the conversion factor is 0.214 mm ps^{-1} . Multiple scattering effects are studied by observing the extra distance travelled by the photons compared with the physical distance across the medium. The 10 ps time resolution corresponds to a spatial resolution of 2.14 mm in the tissue.

2. Modelling light transport in tissue

The measured attenuation of light across the head is a complex function of detector and transmitter geometry, head shape and the scattering and absorption properties of the tissues. Let us assume that the attenuation, in optical density, can be expressed as a modified Beer-Lambert equation

$$\text{Attenuation(OD)} = -\log(I/I_0) = B\mu_a d_p + G \quad (2)$$

where I is the transmitted intensity, I_0 the input light intensity, B is a pathlength factor dependent upon the absorption and scattering coefficients μ_a and μ_s and the scattering phase function; G is an unknown geometry dependent factor, and d_p is the inter-optode distance between source and detector, i.e. the smallest value possible in equation (1).

The validity of equation (2) will depend on how much B varies with the attenuation and scattering coefficients and phase function. It is this question that is addressed in this paper.

To investigate the relationship between attenuation and the transit time of light pulses through tissue, a Monte Carlo model of light transport in tissue has been used (van der Zee and Delpy 1987). This model incorporates an experimentally measured scattering phase function for *in vitro* rat brain measured at 783 nm (van der Zee and

Delpy 1988). The broadening of a spatial delta function input beam of light as it passes through a scattering medium is normally described by the point spread function (PSF). In a similar manner the temporal distribution of light intensity resulting from a spatial and temporal delta function input as it passes through a scattering medium may be described by the temporal point spread function (TPSF). This TPSF will vary with exit position. The TPSF referred to in this paper is integrated over the exit surface area and all exit angles. We implicitly assume in the following that this function is radially symmetric. It should be noted that the origin of the time axis occurs as the light pulse first enters the scattering medium. In this study, the integrated TPSF was modelled for a tissue slab of 1 cm thickness. In the literature, absorption coefficients are usually quoted to base 10 because of the relation to optical density, whilst scattering coefficients are usually to base e, because of their probabilistic definition. Although potentially confusing this is the convention adopted here. Absorption coefficients (base 10) of 0.456, 0.334, 0.263, 0.217, 0.0867 and 0.0434 cm^{-1} and scattering coefficients (base e) of 100, 80, 60, 40 and 20 cm^{-1} were simulated, encompassing the values quoted in the literature for brain tissue (Svaasand and Ellinsen 1983).

Figure 1 shows the calculated attenuation in OD as a function of absorption coefficient for several different scattering coefficients. The simulation is for a delta function input beam at normal incidence. Transmitted light is integrated over the exit surface. The attenuation can be seen to be a non-linear function of absorption, the greatest deviation from linearity occurring at low absorption and high scattering values. This and the normally unknown geometry factor preclude the use of a simple pathlength factor B for a given scattering coefficient. However, in most *in vivo* spectroscopy measurements, one is interested in relating a *change* in a measured attenuation to a *change* in absorption. For this purpose the slope, $\delta\text{OD}/\delta\mu_a$ over the chosen range of scattering and absorption coefficients is required. This parameter we will call the differential pathlength factor, or DPF.

Figure 2 illustrates the modelled integrated TPSFs for a scattering coefficient of 60 cm^{-1} and absorption coefficients of 0.0434, 0.217 and 0.456 cm^{-1} , respectively. It

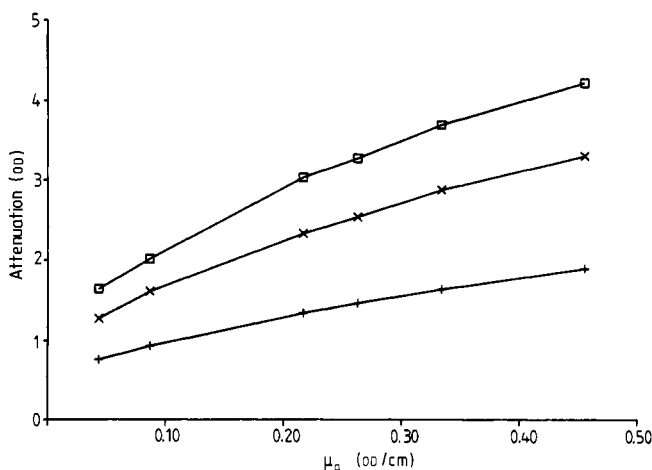


Figure 1. Monte Carlo simulation of attenuation against absorption for light transmitted through a 1 cm slab of brain tissue. Scattering coefficients: +, 20 cm^{-1} ; x, 60 cm^{-1} ; □, 100 cm^{-1} .

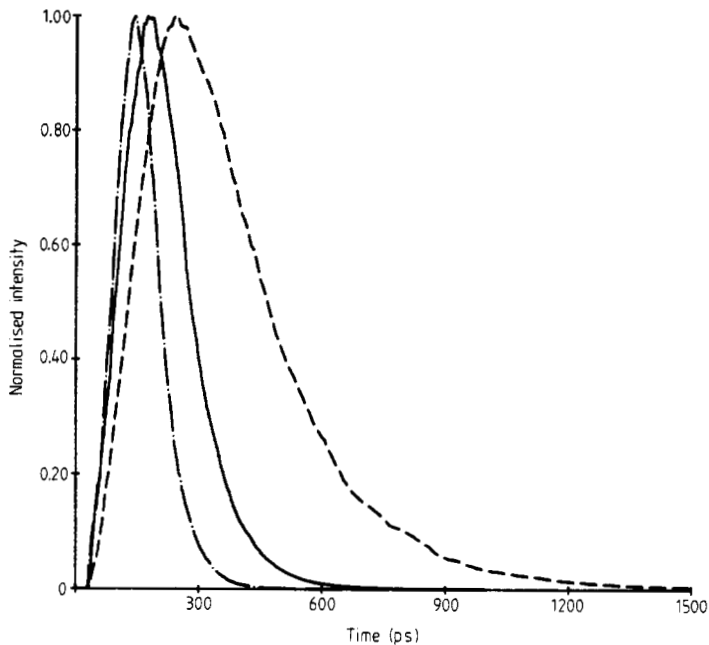


Figure 2. Monte Carlo simulation of the integrated time point spread functions (TPSF) resulting from a normally incident delta function input pulse transmitted through a 1 cm slab of brain tissue. The simulation is for a scattering coefficient of 60 cm^{-1} and absorption coefficients of: - - -, 0.0434 cm^{-1} ; —, 0.217 cm^{-1} ; — · —, 0.456 cm^{-1} .

can be seen that there is considerable time dispersion of the pulse and hence a variation in the pathlength of the detected light. The question therefore arises as to whether some parameter, derived from the integrated TPSF, can be found to correlate with the DPF. Using the Monte Carlo data, the change in transmitted intensity (in optical densities) corresponding to known changes in absorption coefficient has been calculated, and its correlation with the integrated TPSF examined. The integrated TPSF for each data point was analysed and the pathlengths equivalent to the mean of the profile and the 5%, 25%, 50%, 75% and 95% of cumulative intensity calculated. Both the mean and the 50th percentile were found to correlate well with the DPF. The mean was chosen to make it easier in the future to include higher moments in a more sophisticated analysis of the TPSF. The result for the mean is illustrated in figure 3(a).

3. Model verification

The model predictions were verified on a tissue phantom composed of polystyrene-latex particles in water and an infrared absorbing dye using the experimental system shown in figure 4. A mode locked krypton ion laser (Coherent K3000) produces ~ 100 ps pulses at a repetition rate of 76 MHz. These were used both to trigger the synchroscan streak camera (Hamamatsu C1587, M1955), and to pump the ultrafast dye laser (Coherent CR701-3 with Oxazine 750 dye). The output pulses from the dye laser had an autocorrelation width of 6 ps. A beam splitter and monomode optical fibre took a time reference to the edge of the streak camera entry slit, with a variable time delay. The main beam was adjusted to enter the centre of the streak camera entry

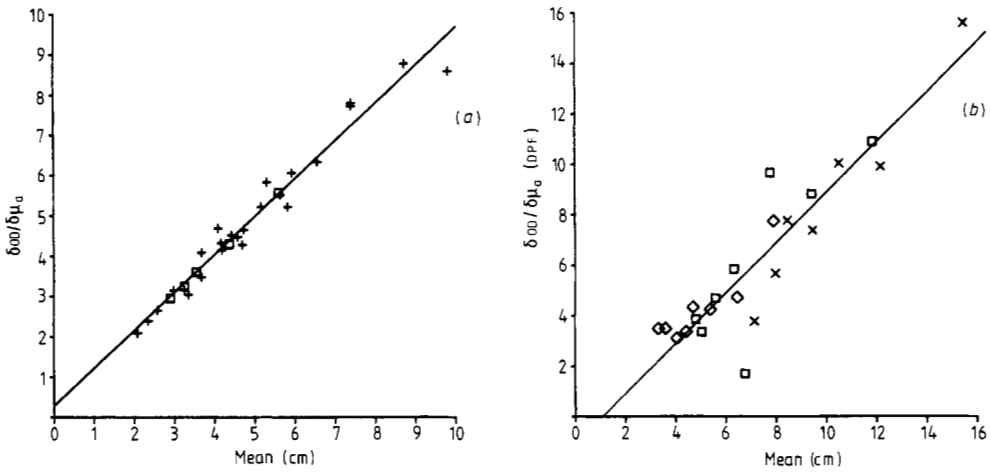


Figure 3. A comparison of modelled and measured phantom results. (a) The mean of the integrated TPSFs is expressed as an equivalent distance in centimetres using equation (1) and a refractive index of 1.4. +, data generated with the brain scattering phase function for $\mu_s = 20, 40, 60, 80, 100 \text{ cm}^{-1}$ and $\mu_a = 0.0434, 0.0867, 0.217, 0.263, 0.334, 0.456 \text{ cm}^{-1}$. The full curve is the regression line, with a slope of 0.94 ± 0.04 and an intercept of 0.28 ± 0.20 . □, data generated with the scattering phase function of the phantom material for a scattering coefficient of 60 cm^{-1} and absorption coefficients of $0.043, 0.0867, 0.217, 0.263, 0.334, 0.456 \text{ cm}^{-1}$. (b) The DPF plotted against the mean of the integrated TPSF for the phantom. The original mixture (x) contained 2.5% by volume of $1.0 \mu\text{m}$ diameter polystyrene latex spheres, and 6.7% by volume of $0.05 \mu\text{m}$ diameter particles, suspended in water. The other concentrations were obtained by 50% (□) and 25% (◇) dilution of this mixture. The full curve is the regression line with a slope of $1.00 (\pm 0.10)$ and an intercept of $-1.08 (\pm 0.77)$. The DPF was calculated by dividing attenuation change by absorption coefficient step. The mean value plotted is the average value of the two integrated TPSFs on either side of the step.

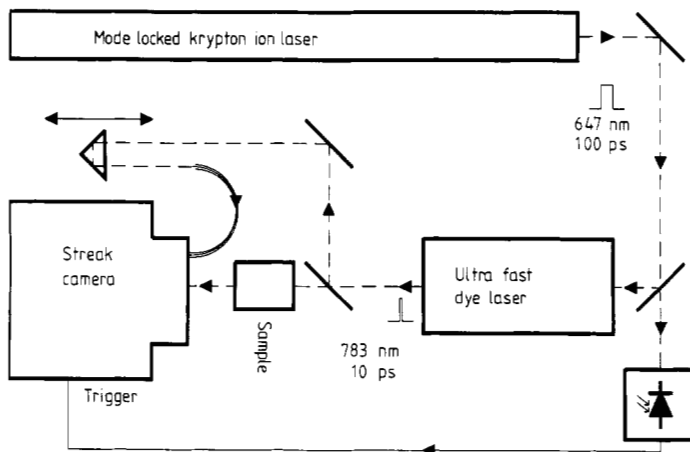


Figure 4. Experimental apparatus for the measurement of integrated TPSFs.

slit. Samples were placed in the main beam and the TPSFs recorded by averaging 128 TV frames. Integrated TPSFs were calculated by summing over the area of the streak camera slit, excluding the time reference. The spatial variation of the TPSF had a full width half maximum less than the 12 mm entry slit size for the sample with maximum scattering and minimum absorption. The input power of the beam was monitored continuously (Coherent 212). Sample attenuation by the phantom was measured using a 1 cm² area silicon photodiode (RS Components) placed against the exit side. To correspond with the Monte Carlo model, a cell of 1 cm thickness and a wavelength of 783 nm were employed.

Two sizes of particles were used in the phantom in an attempt to reproduce the scattering phase function of brain tissue. The diameters of the particles were 1.00 μm ($\pm 0.03 \mu\text{m}$) and 0.05 μm ($\pm 0.002 \mu\text{m}$). The absolute concentrations used gave integrated TPSFs in the range of the Monte Carlo model and the *in vivo* experiments (see later). Variation in scattering coefficient was performed by volumetric dilution of the mixture. The original mixture contained 6.7% by volume of the smaller particles and 2.5% by volume of the larger particles. The total volume of phantom material was 40 ml. Absorption changes were obtained by adding 0.3 ml aliquots of concentrated infrared dye solution (ICI S109564), producing steps in absorption coefficient of 0.053 cm⁻¹ up to 0.424 cm⁻¹, i.e. about three times the expected *in vivo* value (Cope *et al* 1988). Experimental results are shown in figure 3(b), and can be seen to be in reasonable agreement with the model predictions. Several explanations are possible for the minor differences between the experimental and modelled results. In particular, the cell size employed is finite (6 cm \times 6 cm), and the acceptance angle and slit width of the streak camera system is limited. Therefore the TPSF cannot be integrated over all space. It is intended to extend the Monte Carlo model to simulate these finite limits. In addition the scattering phase function of the phantom is not identical to that used in the model. The effect of this small difference in phase function was checked by repeating the Monte Carlo calculations for a scattering coefficient of 60 cm⁻¹ using the scattering phase function of the phantom material calculated from Mie theory (Bohren and Huffman 1983). These data are also shown in figure 3(a). The effect of the slight difference in phase function on the relationship is negligible.

4. Optical pathlength in the brain

The implications of the model predictions have been studied in a series of experiments to measure the integrated TPSF for the transilluminated rat brain. Nine adult Wistar rats (mean weight 288 g) were studied. Following anaesthesia (Urethane 36% w/v intraperitoneal, 5 m kg⁻¹) the temporoparietal muscles were reflected, the skull exposed and cleared of residual surface tissue. A tracheostomy allowed easy manipulation of inspired gas concentrations and a femoral artery was cannulated for blood sampling. The animal was placed in front of the streak camera in the sample position shown in figure 4, the head being immobilised in a stereotactic frame. Pulses of light from the dye laser were incident on the skull diametrically opposite the streak camera entry slit. Sample attenuation caused by the rat's head was monitored using a 1 mm diameter optical fibre and photomultiplier tube (Hamamatsu R928) in place of the silicon photodiode used experimentally on the model verification. Measurements were made and arterial blood samples taken with the animal breathing 100%, 21% and 12% oxygen (balance N₂) and 90% oxygen with 10% carbon dioxide. Further measurements were taken immediately upon death by N₂ inspiration, 15 min post mortem and finally

approximately 22 h post mortem. The rat head diameter was measured at the end of each experiment.

Figure 5 shows the integrated TPSFs for one rat (head diameter 15 mm) together with the input pulse at time zero. It can be seen that as predicted by the Monte Carlo model, considerable temporal dispersion occurred due to multiple scattering of the light in the brain tissue. The overall pulse shape and position showed small changes over a wide range of optical absorption caused by variation in average oxygen saturation (i.e. inspired oxygen concentration (FiO_2) = 100% and FiO_2 = 12%) or cerebral blood volume (i.e. when inspired CO_2 concentration (FiCO_2) = 10%). The data for all animals averaged over equivalent states are shown in table 1. The overall mean of the integrated TPSFs is equivalent to a distance travelled of $5.3(\pm 0.3)$ times the head diameter. The means of the integrated TPSFs for post mortem tissue (measured at 20 °C following 22.4 ± 3.7 h storage at 4 °C) were similar to those obtained at an FiO_2 of 100%.

In a final series of studies the effect of the skull on light scattering and on the average pathlength was investigated since it had been conjectured that some transmitted light may be 'guided' through the skull or between dura and skull and hence not traverse the brain tissues. To examine the effect of light scattering by the skull, in one animal small holes (3 mm diameter) were drilled on either side of the skull following the post mortem integrated TPSF measurement. A further time resolved intensity profile was then obtained with the input laser beam incident directly on the brain tissue and the streak camera focused onto the exposed brain at the far side. No significant difference in the time profiles was observable. In another post mortem animal a small section of bone was carefully removed from the top of the skull, and the brain was

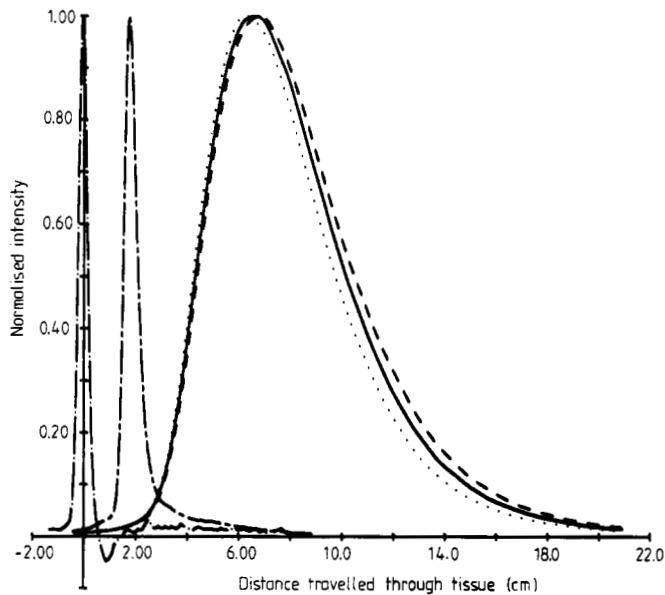


Figure 5. Integrated TPSFs in equivalent distance ($n = 1.4$) measured *in vivo* across a rat head. The input pulse (from the time reference) (— · —) is at the origin and coincides with light first entering the head. Three similar integrated TPSFs show the effect of changes in brain oxygenation. The profiles become narrower as the inspired gas mixture is varied from 100% O_2 (---), through 21% O_2 (—), to 12% O_2 (.....), balance N_2 . This decrease in cerebral oxygenation produced an increase in absorption in brain tissue (deoxygenated haemoglobin absorbs more than oxygenated haemoglobin at 783 nm). The remaining profile (— · —) shows the result with the brain removed and the skull filled with silicone oil ($n = 1.4$).

Table 1. A table of parameters derived from the integrated TPSFs measured experimentally on nine rat heads. The tabulated values are dimensionless. Parameters displayed correspond to the distance ($n = 1.4$) where 5%, 50% and 95% of the total intensity has been received together with the mean, normalised for the distance across the head. The mean distance across the rat heads (including skull) was 1.46 cm (± 0.05). The table shows the values and standard deviations taken over all animals for equivalent states, i.e. the four different inspired gas mixtures and three post mortem states. The final column is an average over all the seven states.

Average (all animals)	100% O ₂	10% CO ₂ 21% O ₂ 90% O ₂ 79% N ₂	12% O ₂ 88% N ₂	0 min	15 min post mortem	22 h post mortem	Average over all data
5th percentile	2.61	2.57	2.55	2.50	2.43	2.60	2.59
50th percentile	5.07	4.98	4.95	4.78	4.60	4.83	4.91
95th percentile	9.62	9.47	9.40	9.04	8.68	8.96	9.23
Mean	5.43	5.35	5.31	5.12	4.93	5.16	5.26
Standard deviation							
5th percentile	0.27	0.25	0.28	0.26	0.24	0.22	0.28
50th percentile	0.24	0.24	0.25	0.25	0.24	0.26	0.31
95th percentile	0.23	0.31	0.28	0.27	0.26	0.34	0.44
Mean	0.23	0.24	0.24	0.24	0.24	0.26	0.31

extracted. The empty skull was then filled with a viscous silicone oil ($n = 1.402$), the bone replaced and the integrated TPSF measured (figure 5). The pulse broadening was $<10\%$ of that observed with the brain present. The possibility of light 'channelling' through the bone of the skull was then checked by replacing the silicone oil with water containing a strong absorber (India ink). Under these circumstances very strong attenuation was observed across the head, greater than 6 optical densities compared with the presence of brain in the skull. It thus appears that the skull and dura make negligible contribution to the integrated TPSF observed across the head.

5. Discussion

The integrated TPSF for the rat head shows the considerable degree of multiple scattering that occurs in brain tissue. The first detected photons to emerge from the head (represented by the point when 5% of the cumulative intensity has been reached) appear on average to have travelled $2.6 (\pm 0.3)$ times the head diameter. The final photons to emerge (the point when 95% of the cumulative intensity has been reached) appear to have travelled $9.2 (\pm 0.4)$ times the head diameter.

The differential pathlength factor derived from the integrated TPSF is 5.3 ± 0.3 times the head diameter. This value is slightly larger than that obtained using the previously described technique of water absorption measurements which was 4.34 ± 0.44 (Wray *et al* 1988). There may be a number of reasons for this discrepancy. First, the time of flight technique relies on a value for the refractive index of brain tissue. The refractive index will lie between the value of 1.33 for water and 1.55 for fat or concentrated protein solutions (Bennett *et al* 1951). The value of 1.4 used in this paper is an estimate based on values reported for rat gut (Gahn and Witte 1986). An accurate value for brain tissue refractive index is being sought. Second, the pathlength factor was measured at 783 nm using time of flight techniques, and between 940 to 1050 nm using the water absorption technique. The results in this paper show that there is a variation in differential pathlength factor with absorption and scattering. The DPF increases with increasing scattering and decreases with increasing absorption. Therefore we would predict the DPF at 975 nm to be lower than that at 783 nm since tissue

absorption is higher at 975 nm and in general scattering decreases with increasing wavelength.

In previous animal studies we have occasionally noted a considerable transient increase in transmitted light intensity upon death. This effect could not be correlated with absorption changes due to blood deoxygenation and blood volume decrease as it has also been observed in fluorocarbon exchange-transfused rats (unpublished observations). In these studies, the observed increase in transmitted light intensity at death was not accompanied by the increase in mean time expected with a simple decrease in absorption. We believe this can only be explained by a decrease in tissue scattering, the cause of which is unknown. The transient increase in transmitted intensity (and associated shortening of the integrated TPSF) persisted only for 1.0–1.5 min after death. The integrated TPSF for the brain tissue 22 h post mortem gave a slightly increased average DPF of 5.5 ± 0.4 , although this value still lay within the range obtained in the living animal.

6. Conclusions

We have introduced the idea of the temporal point spread function (TPSF) of light propagating through tissue together with the differential pathlength factor (DPF) relating changes in measured attenuation to variations in absolute absorption. A Monte Carlo simulation has shown that the mean of the integrated TPSF is in excellent agreement with the DPF. This simulation has been verified experimentally on a phantom with known optical properties. Integrated TPSFs measured across the rat head show a mean value for the DPF of 5.3 ± 0.3 times the head diameter. The maximum variation in the DPF was 0.5 (or 9%) for a wide range of cerebral oxygenation states. The effect of the skull on the DPF is small.

Knowledge of the optical pathlength will permit quantitation of cerebral oxygenation data derived from NIR spectroscopy. Future studies of the way in which the DPF varies with changes in tissue attenuation will further improve quantitation. Additional analysis of the TPSF may also permit direct *in vivo* measurement of tissue absorption and scattering coefficients (Shimizu *et al* 1979) and eventually lead to NIR imaging through tissues (Arridge *et al* 1986, Takiguchi *et al* 1986).

Acknowledgments

This work was carried out with funding provided by The Wellcome Trust, MRC, SERC and Hamamatsu Photonics KK. The authors also wish to thank Dr B Vincent and Dr K Ryan, Department of Physical Chemistry, University of Bristol for the generous supply of polystyrene-latex particles.

Résumé

Estimation du parcours optique dans les tissus par la mesure directe du temps de vol.

La quantification des données spectroscopiques du proche infrarouge dans un milieu diffusant tel que les tissus, nécessite la connaissance du parcours optique dans le milieu. Ce parcours peut maintenant être estimé directement à partir du temps de vol d'impulsions lumineuses de quelques picosecondes. La modélisation par Monte Carlo des impulsions lumineuses dans les tissus a montré que la valeur moyenne du temps des impulsions lumineuses disposées est corrélée avec le parcours utilisé dans les calculs de spectroscopie quantitative. Ce résultat a été vérifié sur fantôme. Les mesures par temps de vol du parcours au travers de la tête de rat donnent un parcours de $5,3 + 0,3$ fois le diamètre de la tête.

Zusammenfassung

Bestimmung der optischen Weglänge in Gewebe durch direkte Flugzeitmessungen.

Die Quantifizierung spektroskopischer Daten im nahen Infrarot in einem Streumedium wie z.B. Gewebe erfordert die Kenntnis der optischen Weglänge des betreffenden Mediums. Diese kann jetzt direkt bestimmt werden aus der Flugzeit von pikosekundenlangen Lichtpulsen. Die Monte Carlo-Simulation von Lichtpulsen in Gewebe hat gezeigt, daß der Mittelwert der Lichtpulse mit der Weglänge korreliert ist, die in quantitativen spektroskopischen Berechnungen verwendet wird. Dieses Ergebnis wurde in einem Phantommateriale verifiziert. Flugzeitmessungen der Weglänge entlang eines Rattenkopfes ergeben eine Weglänge von 5.3 ± 0.3 mal dem Kopfdurchmesser.

References

- Arridge S R, Cope M, van der Zee P, Hillson P J and Delpy D T 1986 Visualisation of the oxygenation state of brain and muscle in newborn infants by near infra-red transillumination *Information Processing in Medical Imaging*, ed. S L Bacharach (New York: Martinus Nijhoff) pp 155-76
- Bennett A H, Osterburg H, Jupnitz H and Richards O W 1951 *Phase Microscopy* (New York: Wiley)
- Bohren C F and Huffman D R 1983 *Absorption and Scattering of Light by Small Particles* (New York: Wiley Interscience)
- Brazy J E, Lewis D V, Mitnick M H and Jöbsis F F 1985 Noninvasive monitoring of cerebral oxygenation in preterm infants: Preliminary observations *Paediatrics* **75**(2) 217-25
- Cope M and Delpy D T 1988 System for long term measurement of cerebral blood and tissue oxygenation on newborn infants by near infrared transillumination *Med. Biol. Eng. Comput.* **26**(3) 289-94
- Cope M, Delpy D T, Reynolds E O R, Wray S, Wyatt J S and van der Zee P 1988 Methods of quantitating cerebral near infrared spectroscopy data *Adv. Exp. Med. Biol.* **222** 183-90
- Delpy D T, Cope M C, Cady E B, Wyatt J S, Hamilton P A, Hope P L, Wray S and Reynolds E O R 1987 Cerebral monitoring in newborn infants by magnetic resonance and near infrared spectroscopy *Scand. J. Clin. Lab. Invest.* **47 Suppl.** 188 9-17
- Ferrari M, Zanette E, Giannini I, Sideri G, Fieschi C and Carpi A 1986a Effects of carotid artery compression test on regional cerebral blood volume, haemoglobin oxygen saturation and cytochrome *c*-oxidase redox level in cerebrovascular patients *Adv. Exp. Med. Biol.* **200** 213-22
- Ferrari M, De Marchis C, Giannini I, Nicola A, Agostino R, Nodari S and Bucci G 1986b Cerebral blood volume and haemoglobin oxygen saturation monitoring in neonatal brain by near infrared spectroscopy *Adv. Exp. Med. Biol.* **200** 203-12
- Fox E, Jöbsis F F and Mitnick M H 1985 Monitoring cerebral oxygen sufficiency in anaesthesia and surgery *Adv. Exp. Med. Biol.* **191** 849-54
- Gahn T and Witte S 1986 Measurement of the optical thickness of transparent tissue layers *J. Microsc.* **141** 101-10
- Hazeki O, Seyama A and Tamura M 1987 Near infrared spectrophotometric monitoring of haemoglobin and cytochrome *aa₃* *in vivo*, *Adv. Exp. Med. Biol.* **215** 283-9
- Jöbsis F F 1977 Non invasive, infrared monitoring of cerebral and myocardial oxygen sufficiency and circulatory parameters *Science* **198** 1264-7
- Piantadosi C C, Hemstreet T M and Jöbsis F F 1986 Near infrared spectrophotometric monitoring of oxygen distribution to intact brain and skeletal muscle tissue *Critical Care Med.* **14** (8) 698-706
- Shimizu K, Ishimaru A, Reynolds L and Bruckner A P 1979 Backscattering of a picosecond pulse from densely distributed scatterers *Appl. Opt.* **18** 3484-8
- Svaasand L O and Ellinsen R 1983 Optical properties of human brain *Photochem. Photobiol.* **38** 293-9
- Takiguchi Y, Aoshima S, Tsuchiya Y and Hiruma T 1986 Laser pulse tomography using a streak camera *Proc. Int. meeting on Image Detection and Quality, Paris, July 16-18*
- van der Zee P and Delpy T 1987 Simulation of the point spread function for light in tissue by a Monte Carlo model *Adv. Exp. Med. Biol.* **215** 179-92
- van der Zee P and Delpy D T 1988 Computed point spread functions for light in tissue using a measured volume scattering function *Adv. Exp. Med. Biol.* **222** 191-8
- Wray S, Cope M, Delpy D T, Wyatt J S and Reynolds E O R 1988 Characterisation of the near infrared absorption spectra of cytochrome *aa₃* and haemoglobin for the non-invasive monitoring of cerebral oxygenation *Biochim. Biophys. Acta* **933** 184-92
- Wyatt J S, Cope M, Delpy D T, Wray S and Reynolds E O R 1986 Quantitation of cerebral oxygenation and haemodynamics in sick newborn infants by near infrared spectroscopy *Lancet* **8515** 1063-1066